New approaches in Electromagnetic Compatibility / Nouvelles approches en Compatibilité Électromagnétique

Field statistics in a one-dimensional Reverberation Chamber model

Ramiro Serra [*], Flavio Canavero

EMC Group, Dipartimento di Elettronica, Politecnico di Torino, C.so Duca degli Abruzzi 24, 10129 Torino, Italy

Available online 17 March 2009

Abstract

This work focuses on building a fairly simple yet physically appropriate 1D model for a Reverberation Chamber which claims to be able to analytically predict the statistical behavior of such a chamber, without forsaking to the benefits of deterministic models. The statistical properties are introduced by varying the size of a 1D stirrer or the cavity size itself. A validation analysis shows agreement with other theories and measured results on real RCs. Field statistics in *undermoded* regime is examined. A radiated emission test is defined and shows reliable matching with reality. The field performance near the conducting walls is investigated. *To cite this article: R. Serra, F. Canavero, C. R. Physique 10 (2009).*
© 2008 Académie des sciences. Published by Elsevier Masson SAS. All rights reserved.

Résumé

Statistiques des champs d'un modèle unidimensionnel d'une chambre réverbérante. Cet article décrit l'élaboration d'un modèle unidimensionnel d'une chambre réverbérante permettant la prédiction analytique du comportement statistique d'une telle chambre, sans renoncer aux bénéfices des modèles déterministes. Les propriétés statistiques sont introduites en faisant varier la taille d'un brasseur unidimensionnel ou bien celle de la cavité elle-même. Ce modèle conduit à des résultats conformes à la théorie et aux mesures effectuées en chambres réelles. Les statistiques des champs en régime sous-modal sont étudiées. Une procédure de teste de la radiation émise est définie et les résultats obtenus sont conformes à la réalité. La performance près des parois conductrices est étudiée. *Pour citer cet article : R. Serra, F. Canavero, C. R. Physique 10 (2009).*
© 2008 Académie des sciences. Published by Elsevier Masson SAS. All rights reserved.

Keywords: Field statistics; Reverberation Chamber; Statistical electromagnetics

Mots-clés : Statistiques des champs ; Chambre Réverbérante ; Électromagnétisme statistique

1. Introduction

A Reverberation Chamber (RC) consists of a metallic shielded room of finite conductivity with a stirring device, antennas, equipment under test, and other devices inside. It formally can be defined as an electrically large, high Q, *multimoded* cavity using mode stirring to create changing boundary conditions in order to obtain a statistically uniform electromagnetic field.

RCs' extensive knowledge up to now, results from a somehow partial juxtaposition of four different approaches: the deterministic models, the statistical models, the empirical techniques and the computer/numerical methods. RCs'

---

* Corresponding author.
 E-mail addresses: ramiro.serra@polito.it (R. Serra), flavio.canavero@polito.it (F. Canavero).

increasing comprehension has evolved from deterministic to statistical models. Both kind of models together provide a reasonable knowledge of the basic principles involved, and help in giving useful guidelines in the construction and/or optimization of an RC. It is not possible to leave one of this approaches behind, as each one of them behaves as a non-exhaustive, non-excluding part of RCs' description. Furthermore, they mutually collaborate to give fairly successful answers in fields where the other one fails, and viceversa. Therefore, there is an obvious gap which makes us change our methodology depending on what kind of result we seek.

1.1. Deterministic models

Deterministic models (i.e. [1,2]) very often start with the abstraction of a reverberation chamber to a simple cavity in order to explain basic, but important concepts such as electromagnetic resonance, the number of modes, and the modal density. As these models move from an ideal cavity into a lossy one, they converge towards a fairly realistic RC, helping in understanding the principles underlying important parameters such as the so called "Lowest Usable Frequency" and the quality factor [3].

Nevertheless, it must be pointed out that an essential constituent of a RC performance is the process of mode-stirring, by which the field distribution inside the cavity becomes a stochastic process. As deterministic models mainly treat a RC as if it were a simple cavity resonator, they do not succeed in describing such processes. Furthermore, the success of deterministic models is intimately linked to the specificity of the chamber geometry.

1.2. Statistical models

On the other hand, statistical models (i.e. [4–6]) frequently start with the presumptions of an *overmoded* cavity. They assist in the analysis where deterministic models fail, like i.e., deriving the probability density functions for each field magnitude, predicting antenna or test object responses in the chamber environment, deriving the spatial correlation function of the fields and some useful expressions for the quality factor.

Obviously they lack of a complete understanding of the chamber, and issues such as the modal density, the proper frequency band for operation, and so forth, are left aside. They frequently start assuming that the modes are "well-stirred" without looking deeper into the conditions leading to this. Furthermore, they often need to assume special geometrical conditions, not quite realistic and somewhat difficult to apply into a specific RC. As an example, the Plane Wave Integral Representation [4] has its rigorous validity only in spherical volumes.

1.3. Empirical techniques

It must be also taken into account that many of the construction suggestions existing in literature were not only derived from applying the mentioned basic physical principles but also in combination with years of practical experience (some examples are [7] and [8]). It is well known how inappropriate and time-consuming is to work under "rule-of-thumb" guidelines (even if successful).

1.4. Fill in the gaps

Consequently, a call for filling this gap and linking the different approximations is needed. This necessity is supported by the aim of having a better understanding, managing a simpler yet complete model and reducing, up to a reasonable minimum, the empirical techniques.

An attempt of filling this gap is introduced in this article, where a one-dimensional RC model is presented. This fairly simple yet physically appropriate model appears to have a statistical behavior equal to real RCs. The solution is found analytically, without forsaking to the benefits of deterministic models.

Section 2 presents the basic 1D RC model with its solution and explains the essential functioning of it. Section 3 presents a validation analysis of the 1D RC model performance by means of a factorial plan technique. Section 4 will compare the 1D RC model with real RCs functioning in *undermoded* regime. Section 5 will compare the performance of the 1D RC model with real RCs, in the case of radiated emission test measurements. In Section 6 the field statistics near the cavity walls will be studied.
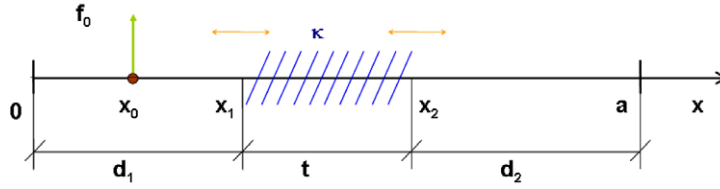
Fig. 1. The one-dimensional cavity under study.

2. The 1D RC model

Our contribution aims at building a model that can be exactly solved, even if it occurs in a case of unrealistic spatial dimensions, i.e., one-dimensional. The 1D models in general are more tractable mathematically and the study of exact results is aesthetically rewarding. They are simple to use, not computationally intensive, and the physical relationship between its main factors (i.e., the frequency, the chamber and stirrer size, the stirrer's complexity, etc.) are easy to understand. The results are often revealing, offering the intuition of how an exact analysis of the real case under study could look like. One-dimensional electromagnetics provide scalar solutions (as opposed to vectorial ones) and some attention should be paid in their analysis. It can be thought as a representation of the behavior of one field component. We shall present further perspectives of the 1D model, which we believe to be useful especially, but not only, for pedagogical purposes.

2.1. The 1D cavity model

The description of our chamber (see Fig. 1 for a schematic diagram) starts as a 1D cavity including a segment of a dielectric material with relative dielectric constant κ inside the vacuum-filled space and a continuous-wave source located at x_0. The length of the chamber is a.

The electromagnetic field inside this chamber obeys the wave equation:

$$\frac{\partial^2 E(x)}{\partial x^2} + \kappa(x)k^2 E(x) = 0, \quad \text{where } \kappa(x) = \begin{cases} 1, & 0 \leqslant x < x_1 \text{ and } x_2 \leqslant x \leqslant a \\ \kappa, & x_1 \leqslant x < x_2 \end{cases} \tag{1}$$

and $k = \omega\sqrt{\mu\epsilon}$ is the free-space wavenumber, μ is the free-space permeability, and ϵ is the free-space permittivity. The $e^{-j\omega t}$ time dependence is suppressed.

The chamber is divided into three regions: d_1 (where the source is), t (the stirrer), d_2 (the Test Volume). One possible set of eigensolutions [3,9] for each region is:

$$E_{n1}(x) = D_n \sin h_n x$$
$$E_{n2}(x) = A_n \sin l_n(x - x_1) + B_n \sin l_n(x - x_2)$$
$$E_{n3}(x) = C_n \sin h_n(a - x), \tag{2}$$

where subindexes 1, 2, 3 mean the region of validity of each expression and n is the modal index. The proposed solution automatically satisfies the boundary conditions at the perfectly conducting "walls" of the chamber in $x = 0, a$. The coefficients A_n, B_n, C_n, D_n and the wave numbers l_n and h_n are determined knowing that at $x = x_1, x_2$, both E and H must be continuous, and that a source is present in $x = x_0$.

The eigenvalues may be obtained as in [3] considering that the equations describing propagation along the x direction of our chamber are equivalent to an appropriate transmission-line circuit, resulting in:

$$h_n^2 \tan l_n t + h_n l_n \tan h_n d_2 + l_n h_n \tan h_n d_1 - l_n^2 \tan l_n t \tan h_n d_1 \tan h_n d_2 = 0 \tag{3}$$

From (1) it is possible to derive the dispersion equation: $h_n^2 - l_n^2 = (1 - \kappa)k^2$ from where, together with Eq. (3), the wave numbers l_n and h_n can be known by means of numerical evaluation as described in [3].

Fig. 2(a) shows the modification of field distribution inside the chamber, due to a change of the κ value in the dielectric region, assumed to maintain a constant ratio $t/a = 0.1$. From the observation of Fig. 2(a), where the real part of the electric field inside the chamber for $\kappa = 1$ (i.e., absence of dielectric) and $\kappa = 1.2$, it is evident that the
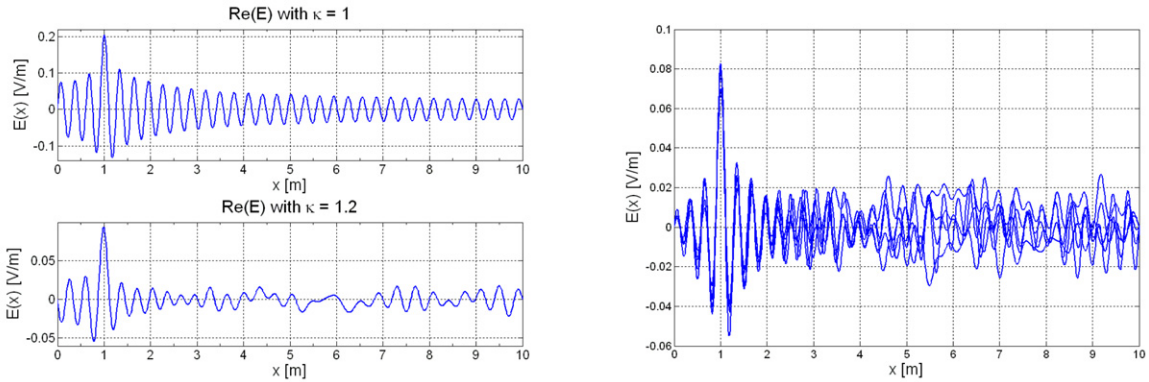
(a) The real part of E inside the 1D cavity model when $\kappa = 1$ and $\kappa = 1.2$.

(b) The real part of electric field E inside the 1D cavity model for 5 different values of the stirrer size.

Fig. 2. Effect of the dielectric layer in the field inside the 1D cavity.

main effect of the dielectric layer inside the chamber is to appreciably change the field distribution inside the "Test Volume" region. Thus, an analogy with the stirrer in real RCs can be established. Additional secondary effects are noticed, such as a reduction in the field magnitude and in the number of modes.

2.2. The 1D RC model

Up to now, we have not been solving a RC but a cavity resonator. Here we demonstrate that a suitable variation of selected parameters can turn the cavity into a RC.

The mode expansion of the electric field in the third region is $E_3(x) = \sum_n C_n \sin h_n(a - x)$, where the coefficient C_n can be calculated as described in Section 2.1. Skipping some analytical calculations, the result for coefficient C_n is found to be:

$$C_n = \frac{M_s \sin h_n x_0}{\kappa l_n \sin h_n d_2 (k^2 - h_n^2)} (h_n \cos h_n d_1 \sin l_n t + \kappa l_n \sin h_n d_1 \cos l_n t) \tag{4}$$

where M_s is the magnitude of the current source, and the other parameters were previously defined. It is clear from Eq. (4) that C_n is a function of all the geometrical and electromagnetic parameters of the problem. If we suppose that any of these parameters is a random variable, then C_n is a random variable [10] and the expression $E_{n3} = C_n \sin h_n(a - x)$ is also a random variable.

The central limit theorem [10] states that if the random variables E_{n3} are independent, then under general conditions, the probability density function of their sum

$$E_3 = E_{13} + E_{23} + \cdots + E_{n3} = \sum_n E_{n3} \tag{5}$$

tends to a normal curve as $n \to \infty$ (i.e., if n is sufficiently large).

As in real RCs, proper statistics apply provided that the geometrical and electromagnetic conditions can afford a series of pseudo-random variables E_n that are independent and many.

As an example, let us uniformly vary the stirrer length t. Fig. 2(b) shows the field distribution inside the RC for five values of the stirrer region size $t/a = 0.11, 0.12, 0.13, 0.14, 0.15$. It can be observed that the field is highly coherent in the region where the source is present but, on the contrary, a considerably uncorrelated field behavior develops in our "Test Volume". The results of 500 independent calculations of the electromagnetic field at a fixed measurement position inside the test volume are shown in Fig. 3(a), that presents the histograms of the real and imaginary parts of the electric field with their fitted normal distributions.

The Anderson–Darling Normality Test (A-D) [11] was applied to these values to determine whether the data of the sample is *nonnormal*. The resulting p-values were 0.762 and 0.503 for the real and imaginary part, respectively,
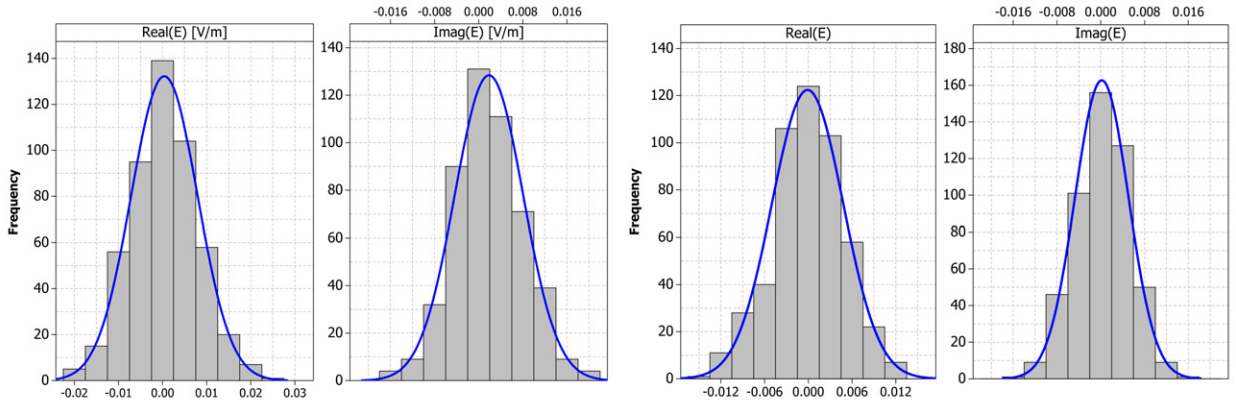
(a) Probability distribution for 500 variations of the stirrer size. (b) Probability distribution for 500 variations of the cavity size.

Fig. 3. Real and imaginary parts of the electric field measured at position $x = 8.5$ m after 500 iterations of two different stirring processes.

thus largely justifying the hypothesis that they follow the normal distribution. These results reproduce the literature findings, i.e., that the field-components distributions match the probability density functions [4,5].

Alternatively, if we solve the cavity without the stirrer region, but we make the chamber length a to randomly vary, we are able to reproduce the behavior of a vibrating-wall chamber [12]. The A-D test was applied resulting in p-values of 0.434 and 0.387, largely justifying again the hypothesis of normality. Fig. 3(b) presents the histograms of the real and imaginary parts of the electric field with their fitted normal distributions.

Many other stirring processes can be studied in analogy of what happens in reality. Factors like the source frequency f_0, the source position x_0, the relative dielectric constant κ, and the factors studied above, are somewhat efficient in the stirring process.

3. Validation analysis

This validation analysis is not meant to validate or justify a specific statistical law for RCs, but to validate the 1D RC model behavior w.r.t. the well-known, worldly recognized, traditional statistical approaches ([4–6]). As several parameters (or "factors") can influence the distribution of the electromagnetic field inside the chamber, in this section, we use a design of experiments technique [13] and define a proper factorial analysis to study the effects of the following geometrical factors:

$$F_1 = \frac{t_0}{a}, \quad F_2 = \frac{\Delta t}{a} \quad \text{and} \quad F_3 = \frac{a}{\lambda} \tag{6}$$

The actual length t of each stirrer was taken randomly, and obtained using $t = t_0 + 2U(0, \Delta t)$, where $U(a, b)$ stands for the uniform distribution with interval (a, b). The t_0 value is the fixed part of our 1D stirrer, while the Δt value is related to the variational part.

These parameters are defined as dimensionless quantities in order to gain generality. A factorial design was defined, outlining three levels (Low, Medium and High) of variation for every factor. Each level was chosen guided by the empirical experience and they are:

$$F_1 = 0.05, 0.1, 0.15, \quad F_2 = 0.03, 0.06, 0.09 \quad \text{and} \quad F_3 = 3, 30, 60 \tag{7}$$

As in Section 2.2, the A-D test was repeated for the resulting 27 experiments. For each configuration of the factors' levels, we calculated the real part of the electric field for 500 different stirrer sizes t as explained above.

The A-D test was run for all experiments, and Fig. 4 presents the worst three and the best three performances of all, for brevity. A code was added for clarity attaching a $-$, 0 or $+$ symbol whether a factor receives a *Low, Medium* or *High* level, respectively. For the worst cases, the p-values are lower than 0.005, while the best three cases show p-values equal to 0.825, 0.724 and 0.569.

A complete analysis of the three factors indicates a total agreement with the behavior found in practice for RCs and with what is reported in literature. The following considerations represent a summary of our observations:
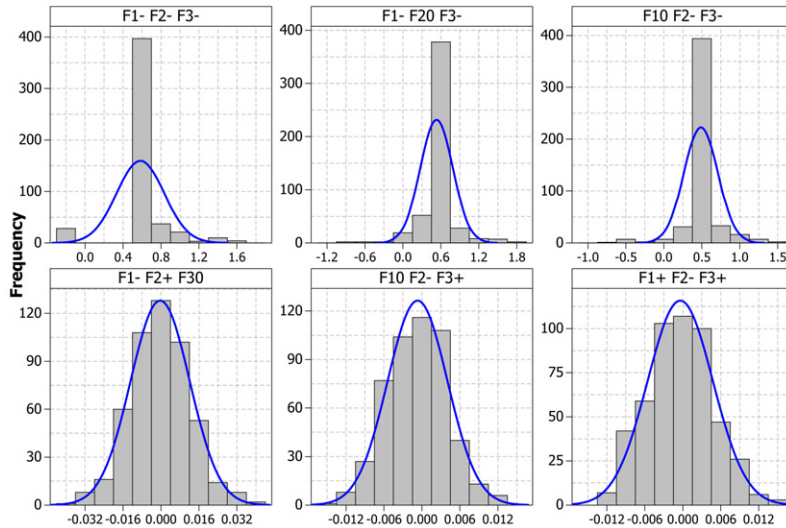
Fig. 4. Histograms and their fitted normal distributions of the worst three and the best three performances out of the 27 experiments of the validation analysis.

– all factors have a main effect on the response;
– the effect of F_3 (indirectly corresponding to the operation frequency f_0) results comparably superior to the rest;
– the effect of every single factor on the response is significantly influenced by the other two factors; thus, a strong interaction is working between them;
– when the frequency is low, no matter how large the change of the stirrer size or variations could be, the performance is not acceptable.

The above properties are in agreement with the published RC theories and with measured results on real RCs. Hence, we can conclude that our 1D model (although simplistic) provides a good representation of reality.

4. *Undermoded* regime

One of the essential conditions for the correct functioning of an RC is that it has to work under an *overmoded* situation. From what has been reported [4,5] and empirically found in measurements, *nonnormal* data distributions correspond to a chamber with a relatively low number of modes present (i.e., the *undermoded* case) and, on the other hand, *normal* data distributions correspond to a chamber with a relatively high number of modes present (i.e. the *overmoded* case). Unfortunately, the question about when does a chamber exactly start to be in an *overmoded* regime remains unanswered (only rule-of-thumb techniques are provided to estimate it, as in [14]).

Important contributions on this subject are found in [15] (and references therein), where theoretical first-order probability density functions are derived for the electromagnetic fields inside RCs. It basically uses the deviations of some physical characteristics of the fields in *undermoded* RCs, from those for ideal reverberation. In [16] the Weibull distribution is proposed to model the distribution of the magnitude of the electric field component. The overall behavior of the fields described by these models is mainly to vary from χ_6^2 and χ_2^2 (i.e., exponential) distributions as the frequency of operation approaches the LUF. It is known that the Weibull distribution is a two-parameter distribution, with a shape parameter k and a scale parameter λ [10]. We will demonstrate in the following, that our 1D RC model can reproduce the main literature findings in this area.

Fig. 5(a) shows the histograms of the absolute value of the electric field with their fitted Weibull distributions, calculated at a fixed measurement position inside the test volume after 500 independent calculations as in Section 2.2. The six panels of Fig. 5(a) correspond to $F_3 = a/\lambda = 5, 10, 15, 50, 100, 200$ (F_3 is defined in Section 3, and λ refers to the wavelength of the source $\lambda = c/f_0$, not to the scale parameter of the Weibull distribution). Of the values chosen for F_3, three refer to an *undermoded* regime and three to an *overmoded* one.

Fig. 5(b) shows the empirical cumulative density functions (CDF) of the previous histograms.

(a) Probability distributions   (b) Cumulative density functions.
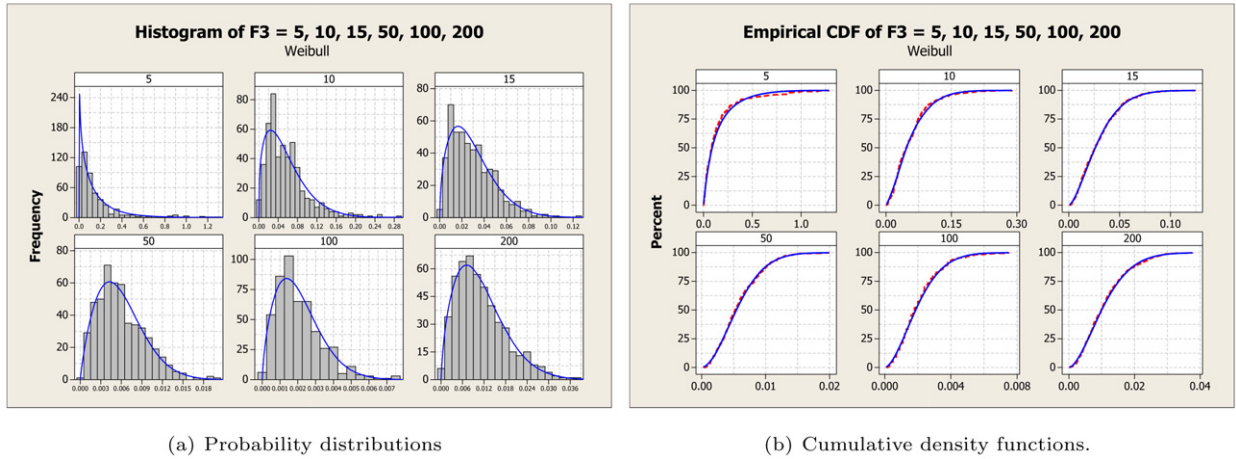
Fig. 5. Absolute value of the electric field with their fitted Weibull distributions at a fixed measurement position inside the test volume for three *undermoded* and three *overmoded* regimes.
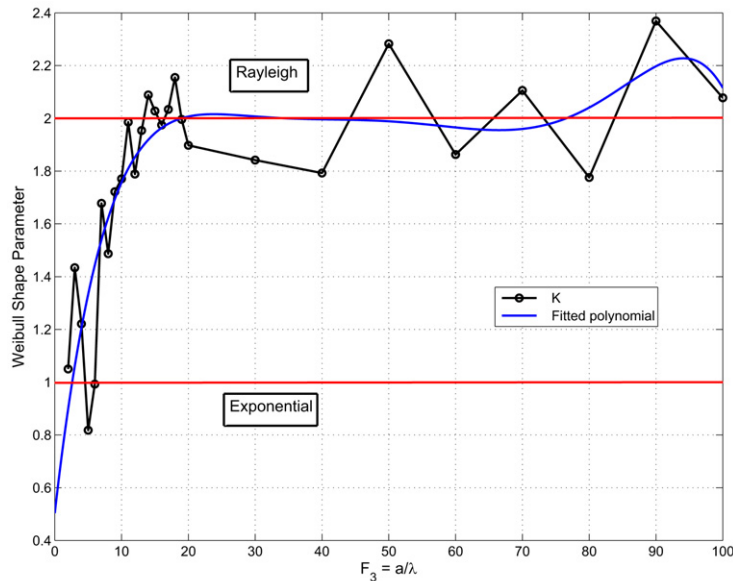

Fig. 6. *k* shape parameter of the Weibull distribution fitting the data calculated from 500 independent variations of the stirrer size.

It can qualitatively be seen that the Weibull distribution gives a very good and smooth approximation of the *under-moded*-to-*overmoded* regimes transition. Fig. 6 shows the shape parameters k for values of $F_3 = a/\lambda$ ranging from 2 up to 100. It can be seen that the overall behavior is to converge towards a Rayleigh distribution ($k = 2$) from the exponential one ($k = 1$). To make it easier to see, a fitted polynomial line was added to the curve.

All of the above is in excellent correspondence of what is reported in [15] and [16].

5. Radiated emission (RE) measurements

In this section, the measurement of the total radiated power of an equipment under test (EUT) in a RC will be addressed. Reference [14], Annex E (and references therein) report how to determine the total radiated power. The main findings in RE tests within RCs, are (not exhaustively) summed up to be:
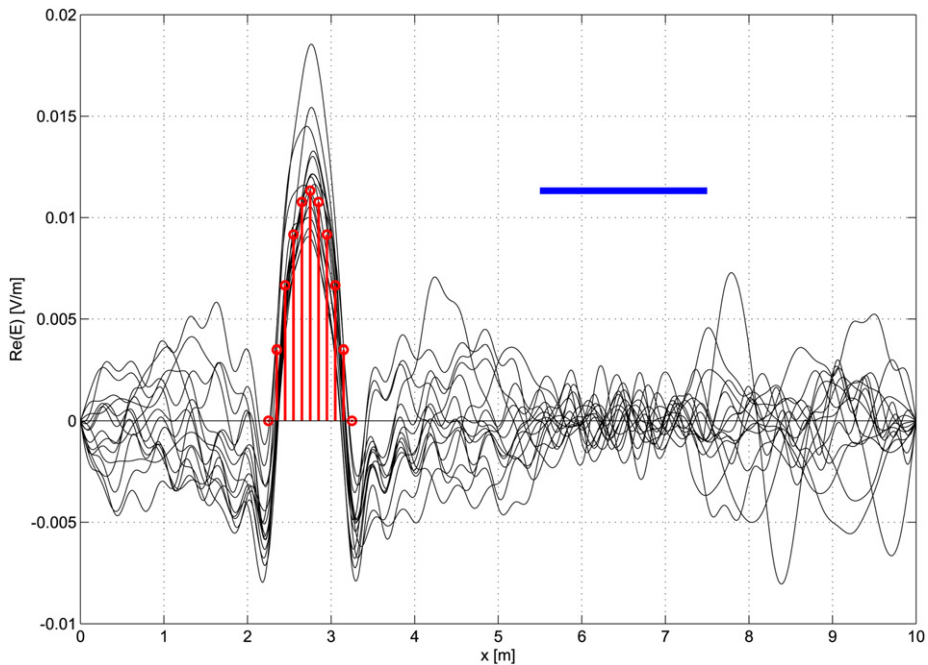
Fig. 7. Real part of the electric field for 15 different stirrer sizes and a 1D EUT. The largest size and the position of the stirrer is depicted by the thick line ($x_1 = 5.5$ m, $x_2 = 7.5$ m), while the distribution of the current sources is represented by the vertical arrows (the scale of current is not provided).

- The RE measurement is independent of the EUT and receiving antenna position, orientation and radiation pattern;
- The averaged and/or maximum power received by an antenna is directly proportional to the averaged and/or power radiated by an equipment under test;
- The main factors influencing this proportionality are: the chamber quality factor Q, the antenna efficiency, the loading and the cavity losses.

The aim of this article is about the assessment of our 1D model to reproduce the main literature findings regarding RCs knowledge.

5.1. Modeling of a test setup

Firstly, we will place a 1D EUT inside the chamber, and study the statistical characteristics when the mode-stirring process is acting. The 1D EUT is modeled as a set of point sources, each one of them as shown in Fig. 1 but with a (discrete) current distribution following that of a dipole. The choice of a dipole as an EUT is supported by the fact that the latter is the most representative of the standard EUT behavior. In fact, [14] recommends to use a *directivity* of $D = 1.7$ (that is to say, a dipole) in the case of RE testing, if the actual *directivity* of the EUT is unknown.

The electric field is then calculated as in Section 2 and the set of sources is superimposed. Fig. 7 shows the real part of the electric field for 15 different stirrer sizes. The largest size and the position of the stirrer is depicted by the thick blue line ($x_1 = 5.5$ m, $x_2 = 7.5$ m), while the distribution of the current sources is represented by the vertical red arrows (the scale of current is not provided). The 1D EUT's length is $L = 1$ m and the frequency $f_0 = 1$ GHz (resulting in a wavelength of $\lambda = 30$ cm, approximately). The chamber's length $a = 10$ m. The process of mode stirring is analogously revealed as in 2 and it is confirmed that the correct statistical behavior is again reproduced.

5.2. RE test procedures

In order to verify the overall performance of this test setup, we will firstly make use of a proper factorial design. We will assess the influence and main effects of three factors: the length of the EUT (L), the power delivered to the

EUT (P_t) and the RC's quality factor (Q) over two widespread known outputs, viz.: the average and the maximum received power. Secondly, the existing relation between transmitted and received power is discussed.

5.2.1. *Assessment of the effect of L, P_t and Q in RE tests*

A factorial design was defined, outlining two levels (Low and High) of variation for every factor. Each level was chosen guided by the empirical experience and they are:

$$L = 1 \text{ m}, 2 \text{ m}, \quad P_t = 1 \text{ W}, 4 \text{ W} \quad \text{and} \quad Q = 100, 1000 \tag{8}$$

The average and maximum of $|E|^2$ (which is proportional to the received power) within the test volume were calculated for the resulting 8 experiments. For each configuration of the factors levels, 500 independent calculations were realized as described in Section 2. The other factors, such as the chamber length, and the frequency of operation were taken to be the same as those of Fig. 7.

A complete analysis of the factors indicates a total agreement with the behavior found in practice for RCs and with the literature. The following considerations represent a summary of our observations:

– it is seen that the radiated emission tests are independent of the EUT size;
– the effect of Q is largely greater in the case of maximum received power (evidencing the higher uncertainty of this method with respect to the average received power);
– the effect of P_t is significantly lower in the case of average received power (supporting the fact that this method needs a more sensitive measurement system to get an accurate result).

The above properties are in agreement with the published RC theories and with measured results on real RCs (in particular, see [14]).

5.2.2. *Determining radiated power*

Reference [14] Annex E, reports how to determine the power radiated from a device using either the average or the maximum received power. In both cases, P_t is calculated to be proportional to the measured average (P_{AveRec}) or maximum power (P_{MaxRec}) with a constant of proportionality found during a necessary calibration campaign.

The equations in (9), given in [14], are used for the mentioned estimation.

$$P_{\text{Radiated}} = \frac{P_{\text{AveRec}} \cdot \eta_{T_x}}{CCF}, \qquad P_{\text{Radiated}} = \frac{P_{\text{MaxRec}} \cdot \eta_{T_x}}{CLF \cdot IL} \tag{9}$$

where CCF is the chamber calibration factor, CLF is the chamber loading factor, IL is the chamber insertion loss, P_{AveRec} is the received power averaged over the number of stirrer steps, P_{AveRec} is the maximum power received over the number of stirrer steps and η_{T_x} is the antenna efficiency factor.

We can reproduce the same test setup using the experiments described in Section 5.2.1, and pretend that the experiments for $P_t = 1$ W are the ones for calibration. Also, we assume the EUT length $L = 1$ m. We computed $|E|^2$ for two different positions within the test volume and for 500 variations of the stirrer. By this process, we are able to determine CCF, whose value is 7.8644×10^{-5}. Afterwards, we apply Eq. (9) to the data of the same experiment but with $P_t = 4$ W. For the resulting P_{Radiated} values using the received mean power method at two different measurement positions, we obtained 4.35 W and 3.64 W (a value of $\eta_{T_x} = 1$ was assumed for the receiving antenna efficiency). The same procedure was repeated for the maximum received power for all the 8 experiments of Section 5.2.1 and for two different positions inside the test volume. The complete list of all the exact results is omitted here for brevity, but they were found to lay between ~ 3.5 W and ~ 4.5 W, except for the cases with $Q = 100$ and with the maximum received power method. These results are reasonably close to the actual $P_t = 4$ W of our forged "unknown" EUT.

Hence, we can conclude once more that our 1D model (although simplistic) provides a good representation of reality.

6. Field statistics near the cavity walls

Observations of mode-stirred chambers has suggested that proper statistics apply, provided that the distance from the walls (or any other conducting structure) is greater than one quarter of the free-space wavelength [14]. To show
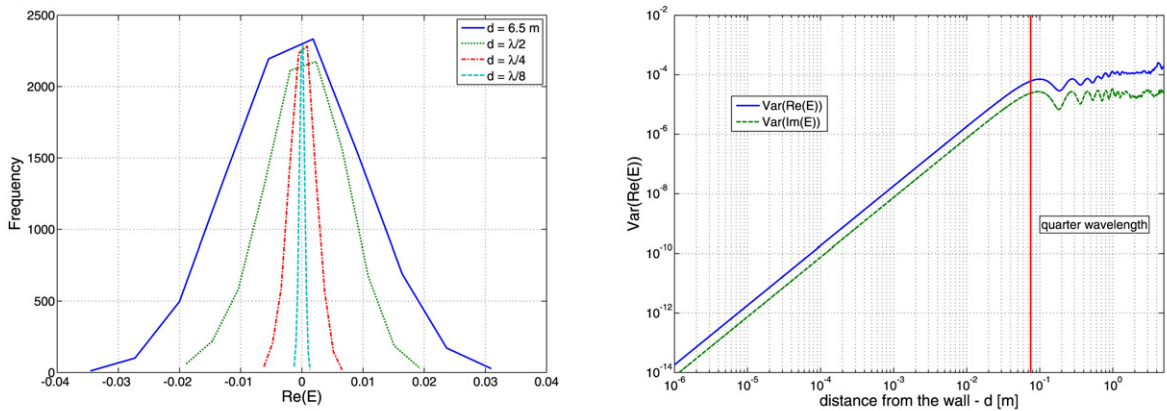
(a) Distributions of the real part of the electric field at different distances from the wall.

(b) Variances of the real and imaginary part of the electric field as a function of the distance from the wall, in logarithmic scale.

Fig. 8. Field statistics near the cavity wall.

the coherence of this "quarter wave rule" between real RCs and our 1D RC model, we solved many one-dimensional chambers to investigate the variation of statistical distribution with position in a cavity. The chamber length $a = 10$ m, the frequency of operation $f_0 = 1$ GHz (with the corresponding wavelength of approximately $\lambda = 30$ cm) and the number of independent stirrer sizes $n = 500$ were chosen as the conditions of the experiments.

Initially, some fixed positions were chosen to be $x = 6.5$ m (mid-way across the test volume), $x = 9.85$ m (a half wavelength from the wall), $x = 9.925$ m (quarter wavelength) and $x = 9.9625$ m (eighth of a wavelength): the resulting field distributions of the real part of the electric field are compared in Fig. 8(a). Note that the distributions still resemble a Gaussian curve when the distance is less than a quarter wavelength, but that the variance is dramatically reduced in value.

To look deeper into this phenomenon, we calculated the field statistics for a large number of positions and plotted the value of the variance of the real and the imaginary part of the electric field against the distance from the left wall $d = a - x$. The results are shown in Fig. 8(b) on a logarithmic scale.

It can be seen that this result gives good reason to the "quarter wavelength rule". An explanation of the fall of the variance when $d < \lambda/4$ is that the boundary conditions compel the total electric field (and each one of its contributing modes) to be zero at the side walls.

7. Conclusions

This article describes a 1D RC model that presents a strong behavioral analogy with 3D RCs. It simulates the electromagnetic field distribution inside a theoretical vacuum-filled 1D segment with the presence of a 1D "stirrer" and of losses in the walls. In this model, the statistically uniform field can be obtained in two different ways: either by varying the size of the stirrer, or (in absence of it) by varying the cavity size. Both processes show reliable normality conditions. The effects of the stirrer size and the frequency are in agreement with theory and measurements. Further characteristics of real RCs were compared with our 1D RC model. These are: the field distribution in RCs working in the *undermoded* regime and their statistics (Section 4), radiated emission measurements (Section 5) and the field statistics near the cavity walls. The main convenience of this model consists on giving a self-consistent description of phenomena related to RCs, without gaps on its theoretical development. It offers an intuition of how an exact analysis of the real case under study could look like. Future work (currently under way) involves both the development of a correlation between the real stirrer and its 1D parameters, and a 3D extension of this model.

References

[1] M.T. Ma, Journal of Electromagnetic Waves and Applications 2 (1998) 339–351.
[2] B.H. Liu, et al., Eigenmodes and the composite quality factor of a reverberating chamber, U.S. National Bureau of Standards, Technical note 1066, 1983.

[3] R.E. Collin, Field Theory of Guided Waves, IEEE-Press, New York, 1991.

[4] D. Hill, IEEE Transactions on Electromagnetic Compatibility 40 (1998) 209–217.

[5] J.G. Kostas, B. Boverie, IEEE Transactions on Electromagnetic Compatibility 33 (1991) 366–370.

[6] T.H. Lehman, EMP Interaction Note 494 (1993).

[7] D.A. Hill, National Institute of Standards and Technology (NIST), Technical note 1506, 1998.

[8] M.L. Crawford, G.H. Koepke, National Bureau of Standards (NBS), Technical note 1092, 1986.

[9] P.M. Morse, H. Feshbach, Methods of Theoretical Physics, McGraw-Hill, New York, 1953.

[10] A. Papoulis, Probability, Random Variables, and Stochastic Processes, McGraw-Hill, New York, 1965.

[11] L.C. Wolstenholme, Reliability Modelling: A Statistical Approach, CRC Press, London, 1999.

[12] F.B.J. Leferink, IEEE International Symposium on Electromagnetic Compatibility 1 (1998) 24–27.

[13] D.C. Montgomery, Design and Analysis of Experiments, John Wiley & Sons, 2004.

[14] CISPR/A and IEC SC 77B: IEC 61000-4-21 – Electromagnetic Compatibility (EMC) – Part 4-21: Testing and Measurement Techniques – Reverberation Chamber Test Methods, International Electrotechnical Commission (IEC) International standard, 2003.

[15] L. Arnaut, IEEE Transactions on Electromagnetic Compatibility 44 (2002) 442–457.

[16] G. Orjubin, et al., Statistical Model of an Undermoded Reverberation Chamber, IEEE Transactions on Electromagnetic Compatibility 48 (2006) 248–251.